THE JOURNAL OF BIOLOGICAL CHEMISTRY VOL. 285, NO. 53, pp. 41455–41462, December 31, 2010

Conserved Residues within the Putative S4–S5 Region Serve Distinct Functions among Thermosensitive Vanilloid Transient Receptor Potential (TRPV) Channels*[S]

Received for publication, May 17, 2010, and in revised form, September 30, 2010 Published, JBC Papers in Press, November 2, 2010, DOI 10.1074/jbc.M110.145466

Stepana Boukalova, Lenka Marsakova, Jan Teisinger, and Viktorie Vlachova[1]

From the Department of Cellular Neurophysiology, Institute of Physiology, Academy of Sciences of the Czech Republic, Videnska 1083, 142 20 Prague 4, Czech Republic

The vanilloid transient receptor potential channel TRPV1 is a tetrameric six-transmembrane segment (S1–S6) channel that can be synergistically activated by various proalgesic agents such as capsaicin, protons, heat, or highly depolarizing voltages, and also by 2-aminoethoxydiphenyl borate (2-APB), a common activator of the related thermally gated vanilloid TRP channels TRPV1, TRPV2, and TRPV3. In these channels, the conserved charged residues in the intracellular S4–S5 region have been proposed to constitute part of a voltage sensor that acts in concert with other stimuli to regulate channel activation. The molecular basis of this gating event is poorly understood. We mutated charged residues all along the S4 and the S4–S5 linker of TRPV1 and identified four potential voltage-sensing residues (Arg^{557}, Glu^{570}, Asp^{576}, and Arg^{579}) that, when specifically mutated, altered the functionality of the channel with respect to voltage, capsaicin, heat, 2-APB, and/or their interactions in different ways. The nonfunctional charge-reversing mutations R557E and R579E were partially rescued by the charge-swapping mutations R557E/E570R and D576R/R579E, indicating that electrostatic interactions contribute to allosteric coupling between the voltage-, temperature- and capsaicin-dependent activation mechanisms. The mutant K571E was normal in all aspects of TRPV1 activation except for 2-APB, revealing the specific role of Lys^{571} in chemical sensitivity. Surprisingly, substitutions at homologous residues in TRPV2 or TRPV3 had no effect on temperature- and 2-APB-induced activity. Thus, the charged residues in S4 and the S4–S5 linker contribute to voltage sensing in TRPV1 and, despite their highly conserved nature, regulate the temperature and chemical gating in the various TRPV channels in different ways.

The vanilloid receptor TRPV1 is a member of the vanilloid subgroup (TRPV) of the transient receptor potential (TRP)[2] channel family that functions as a multimodal signal transducer of noxious stimuli in the mammalian somatosensory system (1). This nonselective cation channel can be activated by noxious thermal stimuli (>43 °C), acidic pH (<6.8) or the alkaloid irritant capsaicin. Moreover, at room temperature (24 °C) and pH 7.3, TRPV1 behaves as a voltage-gated outwardly rectifying channel because it can be activated, in the absence of any agonist, by depolarizing voltages (>60 mV) (2). All of these stimuli act strongly synergistically: capsaicin lowers the threshold for heat activation, capsaicin-evoked currents are augmented by heat or by lowering pH (3), whereas heat, protons, and capsaicin enhance the efficacy and sensitivity of voltage-induced activation (2, 4, 5).

The existence of distinct functional domains through which disparate stimuli converge on the channel protein to open/close its ion-conducting pore is thought to underlie the polymodal nature of not only TRPV1 but also its related, temperature-sensitive, protein family members: heat-activated TRPV2, TRPV3, TRPV4, and cold-activated TRPA1 and melastatin TRP channel 8 (for review, see Ref. 6). Based on the structural similarity to voltage-gated potassium channels, the voltage-sensing domain in these channels is hypothesized to be composed of positively charged amino acids distributed within the transmembrane segments S1–S4 that reorient upon a change in the membrane potential (7, 8). This domain is predicted to be (at least functionally) coupled through the S4–S5 linker helices to the inner helices of the S6 segments which dilate (open) and constrict (close) the pore entryway (9). Indeed, in TRPM8, the charged residues within S4 and the S4–S5 linker form part of the voltage sensor but also critically affect the sensitivity of the channel to chemical and thermal stimuli, indicating that this region might also be involved in the general opening mechanism of the channel (10). In TRPM8 and TRPV1, temperature and agonists shift the voltage for half-maximal activation to less depolarized potentials (2, 11); however, membrane depolarization itself acts only as a partial activator for these two channels and thus probably does not represent the fundamental mechanism for gating (4).

To understand the molecular events by which the S4/S4–S5 linker domain modulates (or translates various stimuli into) the activation gating of TRPV1, we systematically mutated potential voltage-sensing residues all along this region and measured the TRPV1-mediated membrane current responses to voltage, capsaicin, heat, 2-APB, and their combinations. We set out to identify the residues most involved and

* This work was supported by Czech Science Foundation Grants 305/09/0081 and 301/10/1159, Research Project Fund of the Academy of Science of the Czech Republic Grants AV0Z50110509 and GAAV IAA600110701, and by the Ministry of Education, Youth and Sports of the Czech Republic Grants 1M0517, LC554, and GAUK 26110.

[S] The on-line version of this article (available at http://www.jbc.org) contains supplemental Figs. S1–S4.

[1] To whom correspondence should be addressed. Tel.: 420-29644-2711; Fax: 420-29644-2488; E-mail: vlachova@biomed.cas.cz.

[2] The abbreviations used are: TRP, transient receptor potential; TRPV, vanilloid subgroup of TRP family; 2-APB, 2-aminoethoxydiphenyl borate; TRPM, melastatin TRP channel.

clarify whether there is a structural analogy underlying the activation gating in related TRPV2 and TRPV3 channels.

EXPERIMENTAL PROCEDURES

Expression and Constructs of TRPV Channels—HEK293T cells were cultured in Opti-MEM I (Invitrogen) supplemented with 5% FBS as described previously (12, 13). Cells were transiently co-transfected with a cDNA plasmid encoding wild-type or mutant TRPV and GFP (TaKaRa) using the Magnet-assisted Transfection (IBA GmbH) method. rTRPV1 cDNA was kindly provided by David Julius (University of California, San Francisco, CA), hTRPV2 in the pCMV6-XL5 vector was from OriGene Technologies, Inc., and hTRPV3 was kindly provided by Ardem Patapoutian (Scripps Research Institute, La Jolla, CA). Cells were used 24–48 h after transfection. At least three independent transfections were used for each experimental group. The wild-type channel was regularly tested in the same batch as the mutants. The constructs were generated by PCR using the QuikChange XL Site-directed Mutagenesis kit (Stratagene) and confirmed by DNA sequencing (ABI PRISM 3100; Applied Biosystems).

Electrophysiology—Whole cell membrane currents were recorded by employing an Axopatch one-dimensional amplifier and pCLAMP9 software (Molecular Devices). Data were filtered at 2 kHz (−3 dB, four-pole Bessel filter) and digitized at 4–20 kHz. Only one recording was performed on any one coverslip of cells to ensure that recordings were made from cells not previously exposed to high concentrations of agonist.

Experimental Solutions—A system for fast superfusion of the cultured cells was used for drug application (14). The extracellular control solution contained 160 mM NaCl, 2.5 mM KCl, 1 mM $CaCl_2$, 2 mM $MgCl_2$, 10 mM HEPES, 10 mM glucose, adjusted to pH 7.3 and 320 mOsm. In whole cell patch clamp experiments, the pipette solution contained 125 mM cesium gluconate, 15 mM CsCl, 5 mM EGTA, 10 mM HEPES, 0.5 mM $CaCl_2$, 2 mM MgATP, pH 7.3, 286 mOsm. All chemicals were purchased from Sigma-Aldrich.

Quantification of Q_{10} and the Threshold for Heat Activation—The heat-evoked whole cell currents sampled during the rising phase of the temperature ramp were pooled for every 0.25 °C. The absolute current values were plotted on a log scale against the reciprocal of absolute temperature (Arrhenius plot). Temperature coefficients Q_{10} were determined for each cell in the respective temperature range where the Arrhenius plot was linear (correlation coefficient > 0.99) by using the formula: $Q_{10} = \exp(\Delta T \cdot E_a/(R\ T_1\ T_2))$, where R is the gas constant, $\Delta T = 10$ Kelvin, E_a is an apparent activation energy estimated from the slope of the Arrhenius plot between absolute temperatures T_1 and T_2. In wild-type and mutant hTRPV3, temperature coefficients were estimated using the formula $Q_{10} = (I_2/I_1))10/(T_2 - T_1)$, where I_1 and I_2 are the current amplitudes obtained at given temperatures T_1 and T_2. The thermal thresholds for wild-type and TRPV1 mutant activation were measured from the temperatures at which the inward currents plotted on a logarithmic scale declined significantly from a straight line. For this purpose, a stepwise linear regression method was adopted using SigmaPlot 10 software (Systat Software, San Jose, CA).

Statistical Analysis—All data were analyzed using pCLAMP 9.0 (Molecular Devices), and curve fitting and statistical analyses were done in pCLAMP 9.0 and SigmaPlot 10 (Systat Software). No leak subtraction was utilized. Voltage-dependent gating parameters were estimated from steady state conductance-voltage (*G-V*) relationships obtained at the end of 100-ms voltage steps by fitting the conductance $G = I/(V - V_{rev})$ as a function of the test potential V to the Boltzmann equation: $G = ((G_{max} - G_{min})/(1 + \exp(-zF(V - V_{1/2})/RT))) + G_{min}$, where z is the apparent number of gating charges, $V_{1/2}$ is the half-activation voltage, G_{min} and G_{max} are the minimum and maximum whole cell conductance, V_{rev} is the reversal potential, and F, R, and T have their usual thermodynamic meaning. For the quantification of $V_{1/2}$ and the percentage of voltage-independent component of gating from currents obtained in the presence of 10 μM capsaicin (G_{min}/G_{max}), the second capsaicin response was used because: 1) in the wild-type TRPV1, the exponential nature of the desensitization kinetics of the first response to capsaicin, in contrast to the second response, does not allow the achievement of steady-state level during voltage stimulation; 2) in some mutants, the first, but not second, capsaicin response exhibited a substantial slowing down of the activation kinetics, which also did not allow to achieve steady-state voltage responses. All data are expressed as the mean ± S.E. Overall statistical significance was determined by the analysis of variance, if not stated otherwise. When significance was found ($p < 0.05$ or $p < 0.001$), statistical comparisons were performed using Student's *t* test for individual groups.

RESULTS

Identification of Charge-replacement Mutations in the S4–S5 region Inducing Changes in the Voltage-dependent Gating of TRPV1—We individually substituted all charged amino acid residues in the transmembrane segment S4 and the S4–S5 linker of rat TRPV1 and characterized the phenotypes of mutants using whole cell patch clamp recordings from transiently transfected HEK293T cells. The putative structure of this region taken from a homology model published previously (15), and the residues chosen for mutagenesis are depicted in Fig. 1. We also mutated the tyrosine residues Tyr^{554} and Tyr^{555} which have intrinsic dipole moments and thus might theoretically also contribute to voltage sensing (7), three residues (Gln^{560}, Gln^{561}, and Met^{581}) that are known to affect the TRPV1 gating (16), and Gly^{563}, that aligns with the glycine Gly^{573}, mutations of which to Ser or Cys cause defective gating in mouse TRPV3 (17). Previously published homology models for TRPV1 (15, 18), based on the crystal structure of Kv1.2, predict an interaction of Arg^{557} with Glu^{570}, and, another electrostatic interaction within the S4–S5 segment can be inferred for the pair of the two oppositely charged residues spaced about one helix turn apart, Asp^{576} and Arg^{579}. We thus also tested the functional properties of three charge-swapping double mutants, R557E/E570R, D576R/R579D, and D576R/R579E. We hypothesized that if specific interactions between opposite charges are required for proper functioning, the charge-reversing double mutants might functionally rescue the channel.

Voltage-dependent activation properties were initially assessed from the steady-state conductances at different test potentials using 20-mV voltage steps from −120 mV up to +200 mV, first in the extracellular control solution and then in the maintained presence of a saturating (10 μM) concentration of capsaicin preapplied for 5–10 s (until the peak amplitude was reached; Fig. 2*A*). Mutations Y554A, Y555S, E570L, and two charge-reversing mutations, R557E and R579E, led to a complete loss of function. In these mutants, 10 μM capsaicin neither induced measurable currents at a holding potential of −70 mV nor affected voltage-dependent (up to +200 mV) and heat-dependent currents (up to 48 °C; supplemental Fig. S3*B*). Neither of these nonfunctional mutants exhibited significantly higher basal currents at −70 mV compared with nontransfected cells. The Y554F and Y555F mutations produced fully functional channels, indicating that aromatic side chains are required at these positions.

To test whether the residues in the S4/S4–S5 region have a central role in TRPV1 voltage sensing, similar to that suggested for TRPM8 (10), we characterized the conductance-to-voltage (*G-V*) relationships obtained under control conditions in all measurable mutants. Equilibrium properties of activation were calculated from Boltzmann fits to the *G-V* relations. For wild-type TRPV1, the Boltzmann fit gave a half-maximal activation voltage ($V_{1/2}$) of 154 ± 4 mV and an apparent number of gating charges (z) of 0.70 ± 0.01 (n = 59) (Fig. 2, *B* and *C*; supplemental Fig. S1). In six single mutants (R557A, R557L, E570A, D576N, D576R, R579A) and in all the double mutants, the open probabilities were apparently below 0.5 for voltage protocols up to 200 mV, so that values for $V_{1/2}$ and z could not be derived reliably. In contrast, $V_{1/2}$ was shifted toward less depolarizing voltages for R557K (97.1 ± 4 mV; n = 13), G563S (78 ± 2 mV; n = 6), and M581T (122 ± 11 mV; n = 11). No significant changes in z were detected among the measurable mutants (p = 0.492; n = 4–59; supplemental Fig. S1).

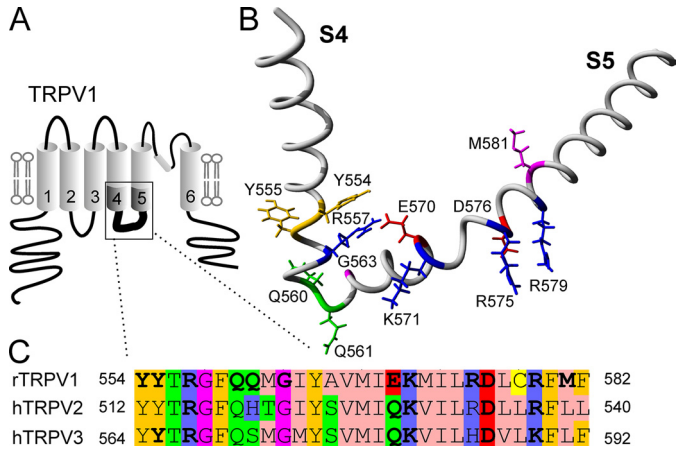

FIGURE 1. **Putative S4/S4–S5 segment of TRPV1.** *A*, sequence comparison of the S4–S5 domain of rat TRPV1 (GenBank accession no. NM_031982) with that of hTRPV2 (NM_016113.3) and hTRPV3 (NP_659505.1). Protein sequences were aligned using MUSCLE multiple alignment software with Zappo score colors. *B*, homology model of the S4–S5 region of rTRPV1 taken from Ref. 15. *C*, residues described under "Results" are indicated in *bold* type.

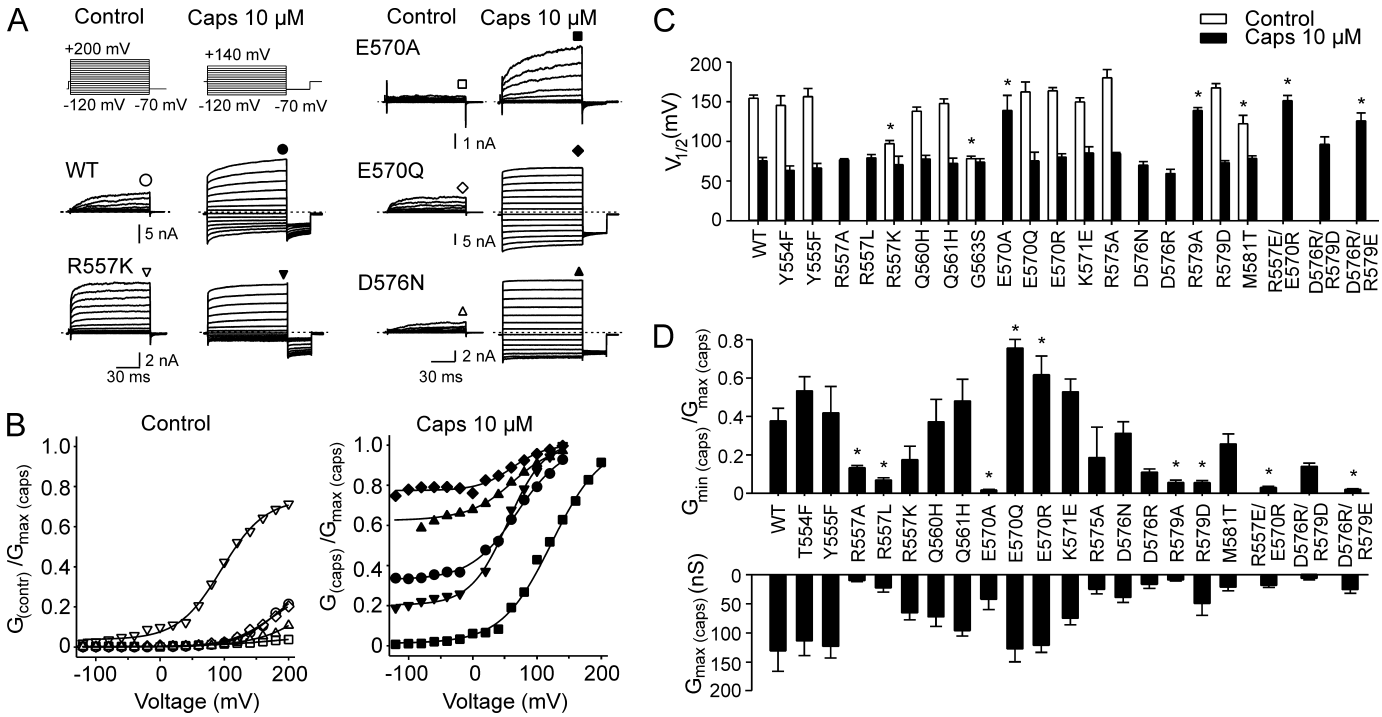

FIGURE 2. **Voltage dependence of TRPV1 mutants.** *A*, representative whole cell patch clamp current traces in response to a family of voltage steps in HEK293T cells transfected with wild-type and TRPV1 mutants in the absence (*open symbols*) or presence of 10 μM capsaicin (*filled symbols*). *B*, representative Boltzmann fits to conductances shown in *A*, obtained from steady-state currents at the end of the pulse (indicated by *symbols* in *A*), normalized to maximal conductance G_{max} in 10 μM capsaicin. *C*, $V_{1/2}$ for wild-type TRPV1 and indicated mutants in the absence (*open bars*) or presence of 10 μM capsaicin (*filled bars*). The *asterisks* indicate significance level. Under control conditions, some mutants did not reach half-maximal activation at voltages up to 200 mV. *D*, summary of voltage-independent component of capsaicin-induced gating (*upward bars*) and G_{max} in 10 μM capsaicin (*downward bars*). Each *bar* is the mean ± S.E. (*error bars*); $n > 4$.

The saturating (10 μM) concentration of capsaicin has been shown to overcome TRPV1 desensitization (19, 20) and reveal the voltage-independent component of TRPV1 gating (4). To characterize further the sensitivity of voltage-induced activation, we quantified $V_{1/2}$ and the percentage of the voltage-independent component of gating from currents obtained in the presence of 10 μM capsaicin (G_{min}/G_{max}). In contrast to control conditions, the *G-V* relations obtained in the presence of the saturating concentration of capsaicin could be fitted for all functional mutants (Fig. 2*C*; supplemental Fig. S1), giving a $V_{1/2}$ of 75 ± 4 mV and z of 0.83 ± 0.06 (n = 18) for wild-type TRPV1. Notably, the three charge-swapping double mutants exhibited measurable voltage-dependent activity, indicating a partial recovery of the functionality of the R557E and R579E mutant channels (Fig. 2*D*; supplemental Fig. S3*B*). Compared with wild-type TRPV1, prominent rightward shifts in $V_{1/2}$ were found for E570A ($V_{1/2}$ of 139 ± 19 mV; n = 5), R579A ($V_{1/2}$ of 139 ± 4 mV; n = 9), R557E/E570R ($V_{1/2}$ of 151 ± 7 mV; n = 6), and D576R/R579E ($V_{1/2}$ of 125 ± 10 mV; n = 9). Significant changes in the apparent gating valence z were detected in E570R (2.1 ± 0.3; n = 6) and D576R/R579D (0.43 ± 0.4; n = 7), indicating that the S4–S5 linker may increase its contribution to voltage sensing when capsaicin is present. Remarkably, R557A, R557L, D576N, D576R, which were only weakly ($V_{1/2}$ > 200 mV) voltage-dependent under control conditions, became as voltage-sensitive as wild-type TRPV1 (p = 0.022; n = 7–18) in the presence of capsaicin, suggesting a preserved or even increased allosteric effect between these two stimuli. Compared with wild-type TRPV1 (38 ± 7%; n = 18), the percentage of the voltage-independent component of capsaicin-induced gating (G_{min}/G_{max}) was strongly (p < 0.01) reduced in R557A, R557L, E570A, R579A, R579D, R557E/E570R, and D576R/R579E. In contrast, this component was predominant in E570Q (76 ± 5%; n = 3) and E570R (62 ± 10%; n = 10).

Mutations in S4/S4–S5 Region of TRPV1 Exhibit Changes in Capsaicin and 2-APB Sensitivity—Our screen of the putative S4/S4–S5 region identified the residues critically involved in the capsaicin- and voltage-dependent activation of TRPV1. Some of the mutations that exhibited significant responses to 1 μM capsaicin at −70 mV had strongly impaired the activation/deactivation parameters (Fig. 3, *A* and *B*). Compared with WT TRPV1, the E570Q mutation accelerated the activation rate (τ_{on}; from 1.3 ± 0.2 s to 0.3 ± 0.1 s; n = 26 and 9). In contrast, a significantly slower rate of activation was observed in R557A (58.7 ± 27.7 s; n = 5), M581T (49.8 ± 12.5 s; n = 8), D576R (45.1 ± 6.9 s; n = 4), Q560H (30.6 ± 8.0 s; n = 6), R557K (8.3 ± 2.0 s; n = 10), and E570R (3.6 ± 0.6 s; n = 6), indicating that these residues contribute to the transduction of the capsaicin-binding signal to the opening of the pore. The estimated deactivation time (T_{50}; the time taken for the current to decrease to 50% of its level before removing the capsaicin) was markedly slowed down in R557K (16.7 ± 1.2 s; n = 11), compared with the wild type (2.2 ± 0.2 s; n = 26), but, remarkably, not in R557A or R557L, indicating that the specific side chain properties of Arg^{557}, and not only a positive charge at this residue, are important for deactivation gating process. In R557A, R557K, Q560H, and M581T, the second response to 1 μM capsaicin reapplied after apparent washout (20 s later or, for R557K, 120 s later) had a faster onset than in the wild type, suggesting that the process of deactivation was incomplete.

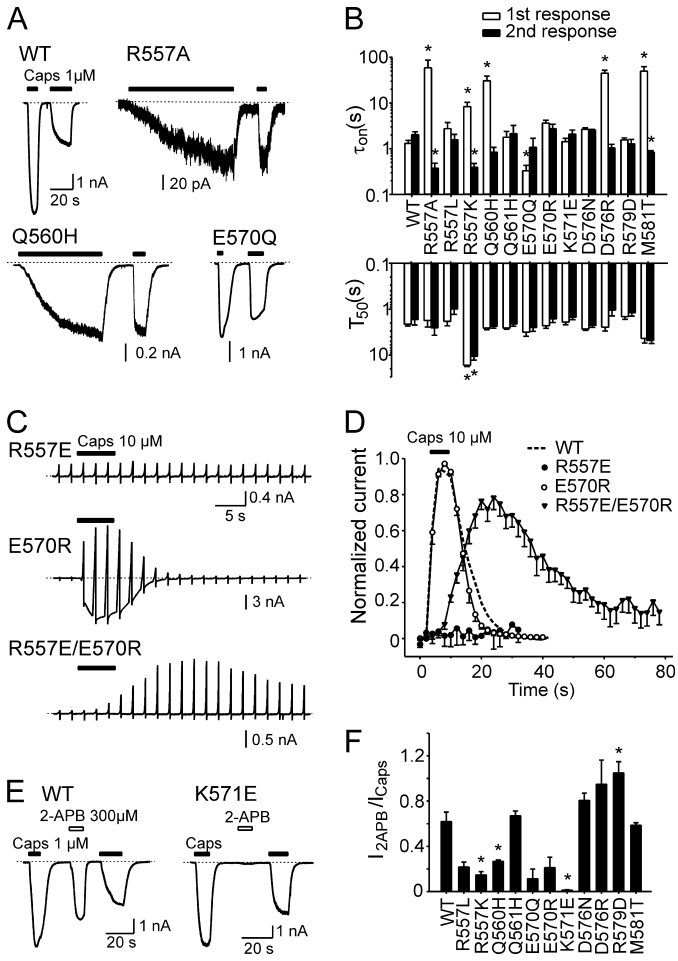

FIGURE 3. **Mutations in S4 and the S4–S5 linker alter chemical sensitivity of TRPV1.** *A*, sample recording of whole cell current responses to consecutive applications of capsaicin (1 μM) at −70 mV. *B*, averaged time constants obtained from monoexponential fit of the onset of first and second capsaicin response and deactivation times (T_{50}) for all measurable mutants. The *asterisks* indicate significance level. *C*, whole cell currents in response to voltage protocol consisting of a 500-ms ramp from −70 mV to +100 mV applied every 2 s in the absence or presence of 10 μM capsaicin. *D*, averaged currents measured at 90 mV constructed from three to five independent recordings such as shown in *C*. The superimposed *dotted line* indicates wild type. Baseline was subtracted. *E*, 2-APB responses reduced by K571E mutation. Holding potential was −70 mV. *F*, mutation effects on 2-APB responses of TRPV1.

To characterize also the activation/deactivation kinetics in mutants barely responding to 10 μM capsaicin at −70 mV, we used a voltage protocol consisting of a 500-ms ramp from −70 mV to +100 mV applied every 2 s and measured whole cell currents at +90 mV before, during 6-s exposure to, and after washout of 10 μM capsaicin (Fig. 3*C*). The time courses of the capsaicin-induced (depolarization-modulated) whole cell currents through R557A, R557L, E570R, D576R, R579A, and R576R/R579D closely resembled those of wild-type TRPV1 (supplemental Fig. S2). In contrast, R557E/E570R exhibited slower activation and deactivation kinetics (Fig. 3, *C* and *D*). A significantly faster offset of capsaicin-dependent responses was detected in E570A and R576R/R579E. Thus,

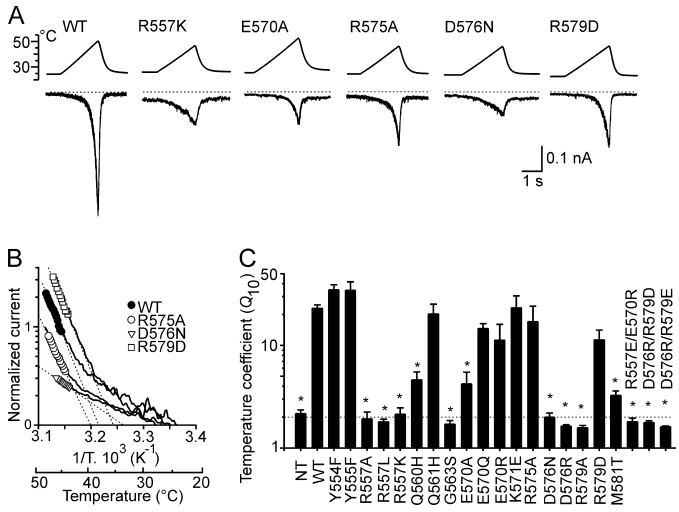

FIGURE 4. **Mutations in S4 and the S4–S5 linker alter temperature sensitivity of TRPV1.** *A*, representative recordings of whole cell current responses to application of 25–48 °C heat ramp (10 °C/s) at −70 mV. *B*, Arrhenius plot of whole cell currents obtained from representative cells shown in *A*, normalized at 25 °C (*ordinate*, log scale) and plotted against the reciprocal of absolute temperature (*abscissa*). Temperature coefficients Q_{10} were determined for each cell over the temperature range where the Arrhenius plot was linear (*dashed lines*). *C*, effects of mutations on Q_{10}. *Dotted line* indicates the value at which the temperature dependence of the thermally induced currents is considered to be nonspecific, *i.e.* close to that of the aqueous diffusion limit (~2). *NT* denotes nontransfected cells. Each *bar* is the mean ± S.E. (*error bars*); $n = 33$ for wild type and 3–15 for mutants.

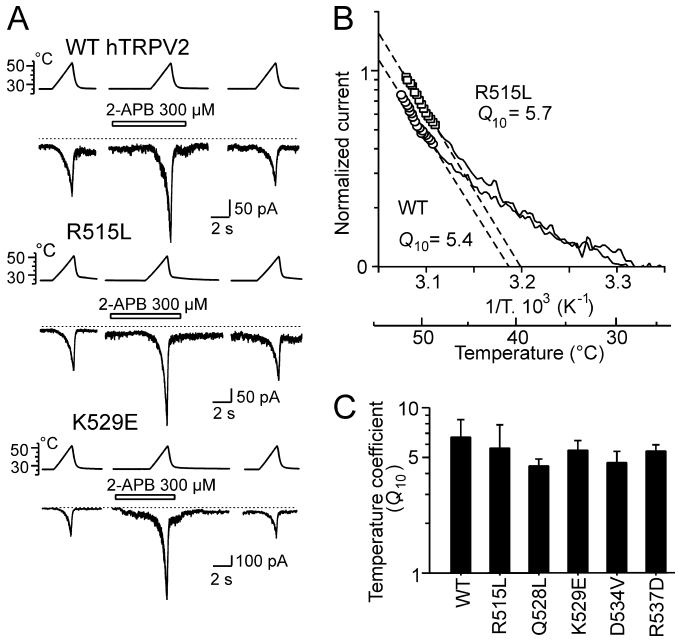

FIGURE 5. **Mutations homologous to those identified in TRPV1 do not alter temperature and chemical sensitivity in hTRPV2.** *A*, representative recordings of whole cell current responses to application of 25–57 °C heat ramp (10–14 °C/s) recorded from cells expressing wild-type or mutant hTRPV2 in the absence or presence of 2-APB (300 μM) at −70 mV. *B*, Arrhenius plot of whole cell currents obtained from representative cells shown in *A*, normalized at 25 °C. Q_{10} was determined over the temperature range where the Arrhenius plot was linear (*dashed lines*). *C*, summary of Q_{10} determined for wild-type hTRPV2 and indicated mutants. Each *bar* is the mean ± S.E. (*error bars*); $n = 10$ for wild type and 3–6 for mutants.

the mutations that caused similar defects in the voltage dependence affected the chemical sensitivity of TRPV1 very differently.

2-APB is a common activator of TRPV1, TRPV2, and TRPV3 channels (21, 22), and the mechanism of 2-APB sensitivity in TRPV1 and TRPV2 appears to be at least partly distinct from TRPV3 (23). Therefore, we wondered to what extent the substitutions at the sites conserved among the S4/S4–S5 domains of these three proteins affect the 2-APB sensitivity of TRPV1 (Fig. 3, *E* and *F*). Among the mutants that exhibited significant responses to 1 μM capsaicin at −70 mV, the inward currents induced by 300 μM 2-APB were reduced, relative to 1 μM capsaicin, in R557L, R557K, Q560H, E570Q, E570R, and most strongly (>50-fold) in K571E. Taken together, these results characterize the residues involved in capsaicin-dependent activation (Arg^{557}, Gln^{560}, Glu^{570}, Asp^{576}, and Met^{581}) and deactivation (Arg^{557}) and identify Lys^{571} as a residue specifically contributing to 2-APB sensitivity.

Mutations in S4 and S4–S5 linker Alter the Temperature Sensitivity of TRPV1—The temperature coefficient (Q_{10}) for the gating of TRPV1 has been shown to be a very subtle parameter, being highly susceptible to mutations at vital domains of the TRPV1 protein (12, 13, 15). To address the role of the S4/S4–S5 region in the heat-dependent gating of TRPV1, we quantified the temperature threshold for heat activation and the macroscopic Q_{10} for all measurable mutants from the Arrhenius plots of individual current-temperature relationships (Fig. 4; supplemental Fig. S3*A*). At a membrane potential of −70 mV, the mean threshold for the temperature-induced membrane currents measured in the wild-type channel was 41.5 ± 0.4 °C, and the mean Q_{10} calculated for the temperature range 43–48 °C was 23.1 ± 1.8 ($n = 25$) (13).

Among the mutants tested, the most frequently observed phenotype was a leftward shift in the temperature threshold and a reduction in Q_{10}, indicating that these mutants lost their temperature sensitivity. Notably, a significantly higher threshold for heat activation was detected for E570A (44.3 ± 0.7 °C; $p < 0.005$; $n = 19$). The Y554F, Y555F, Q561H, E570Q, E570R, K571E, R575A, and R579D mutations left the Q_{10} and the threshold for heat activation unchanged.

TRPV2 and TRPV3 Mutants Homologous to Those of TRPV1 Are Fully Functional—The high conservation of the S4/S4–S5 domain throughout the mammalian members of the TRPV channel subfamily raises an important question concerning the extent to which the results from TRPV1 could be generalized to other TRPV channels, particularly TRPV2 (72.4% amino acid identity within the S4/S4–S5 region) and TRPV3 (65.5% identity). To explore this issue, we focused on the residues homologous to those found to be important for the activation of TRPV1 (Fig. 1*C*). We constructed five mutants of human TRPV2: R515L, Q528L, K529E, D534V, and R537D, and characterized their activation properties (Fig. 5). Because the equivalent mutations generally led to a loss of temperature dependence in TRPV1, we used the temperature-current characteristics as an appropriate measure of functionality. We applied a stimulation protocol consisting of a 25–57 °C heat ramp (~10–14 °C/s), recorded in the absence and presence of 2-APB (300 μM). In contrast to what has been reported previously (24), we were able to measure specific heat-activated membrane currents in HEK293T cells transiently transfected with wild-type human TRPV2 (threshold

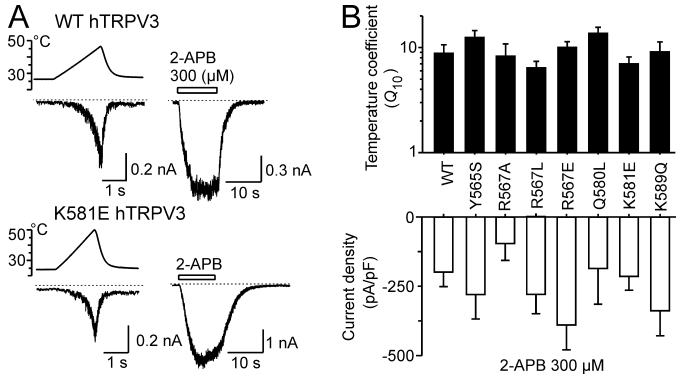

FIGURE 6. **Mutations homologous to those identified in TRPV1 do not alter temperature and chemical sensitivity in hTRPV3.** *A*, sample recording of whole cell current responses to consecutive application of 25–48 °C temperature ramp (10–14 °C/s) and 2-APB (300 μM) in hTRPV3 and K581E-hTRPV3. *B*, summary of Q_{10}- and 2-APB-induced current densities determined for wild-type and mutant hTRPV3. Each *bar* is the mean ± S.E. (*error bars*); $n = 9$ for wild type and 3–7 for mutants. No significant changes were detected ($p = 0.344$).

50.2 ± 0.8 °C; $n = 11$), and these currents were markedly potentiated by 2-APB (2.6 ± 0.4 at 54 °C; $n = 5$). The extent of 2-APB potentiation of the heat-induced currents through TRPV2-K529E was not different from that in the wild-type channel (2.6 ± 0.5; $n = 4$; $p = 0.951$), which was surprising because a homologous mutation led to a loss of 2-APB sensitivity in TRPV1. The Q_{10} values for the TRPV2 mutants were indistinguishable from wild type (Fig. 5*C*; $p = 0.775$), indicating that the temperature sensitivity was also preserved in all mutants tested.

In human TRPV3, we individually mutated residues Tyr^{565}, Arg^{567}, Gln^{580}, Lys^{581}, Asp^{586}, and Lys^{589} (Fig. 1*C*) and examined the temperature-current characteristics and maximal current densities evoked by 300 μM 2-APB at −70 mV (Fig. 6*A*). A rapid heating protocol (25–48 °C; ~10–14 °C/s) was followed by a 10-s application of 2-APB. We found that, except for hTRPV3-D586A, which was nonfunctional, the phenotypes of all of the hTRPV3 mutants were not statistically different from those of the wild type (Fig. 6*B*). Taken together, these data indicate that the mechanism of temperature sensitivity in TRPV1 appears to utilize different residues from those in TRPV2 and TRPV3, and it may be that this is not fully conserved throughout thermosensitive TRPV channels. In addition, neither the hTRPV2-K527E mutation nor the hTRPV3-K581E, corresponding to rTRPV1-K571E, affected the 2-APB-dependent currents, further supporting the recently proposed suggestion that the mechanism of 2-APB activation is not completely conserved among the TRPV1, TRPV2, and TRPV3 channels (23).

TRPV1 Mutation G563S Homologous to Constitutively Active TRPV3 Mutation G573S Also Leads to Overactive Channels—The glycine 563 positioned in the S4–S5 linker of the TRPV1 channel is highly conserved among the members of the TRPV subfamily of TRP channels. A naturally occurring mutation of this glycine in the TRPV3 gene (G573S or G573C) is associated with an inherited form of spontaneous hairlessness and dermatitis (25) and has been attributed to the overactive functioning of TRPV3 channels (17). We were, therefore, particularly curious to see whether the equivalent mutation in rat TRPV1 also leads to spontaneously active receptors. We found that HEK293T cells expressing the G563S mutant of TRPV1 exhibited only slightly enhanced basal activity that amounted to 7.2 ± 3.0% (at 25 °C and at −70 mV) of the current induced by 1 μM capsaicin ($n = 7$; supplemental Fig. S4*A*). In the extracellular control solution, $V_{1/2}$ was shifted toward less depolarizing potentials (78 ± 2 mV; $n = 6$) compared with WT-TRPV1, indicating an enhanced voltage-dependent activity of the TRPV1-G563S mutant at more physiological potentials (Fig. 2*C*; supplemental Fig. S4*B*). Inward currents induced by 1 μM capsaicin exhibited slow activation kinetics and an incomplete deactivation that was fully blocked by 1 μM ruthenium red. Similar to what was discovered for TRPV3-G573 mutants (17), we found that TRPV1-G563S was not responsive to a temperature ramp (from 25 °C to 48 °C; Fig. 4*C*) and was only weakly sensitive to 300 μM 2-APB. These data suggest that mutation G563S stabilizes the open conformation of the channel so that Gly^{563} in TRPV1 could play an analogical role in channel gating as in TRPV3; the extent of spontaneous activity might, however, depend on the TRPV channel specific voltage, chemical, and temperature operation range.

DISCUSSION

There is now mounting evidence that chemical and thermal stimuli interact allosterically through independent molecular mechanisms in thermosensitive TRP channels. Vanilloids interact at intracellular/intramembranous regions in and adjacent to S3 and S4 (26, 27); a small region of the proximal part of the C-terminal domain (Val^{686}-Trp^{752}) renders the TRPV1 channel heat-sensitive, and this region is transplantable into the cold-sensitive TRPM8 channel, whose voltage-induced responses become potentiated by heat (15). Further evidence in favor of mechanistically distinguishable mechanisms of activation was presented for TRPV1 and TRPV3, in which agonist- and temperature-induced activations are separable from other activation mechanisms (23, 28, 29). What is much less clear is the intrinsic mechanism by which thermosensitive TRPV channels are gated by voltage. Given that the S4/S4–S5 domain is strongly conserved among TRPV channels, in particular, the positively charged residue in S4 is completely conserved across TRPV proteins, the new information obtained for TRPV1 may be important in understanding the structure-function relationships in related channels. On the other hand, to date, definitive proof that the S4–S5 region contributes to voltage-dependent gating has been only achieved for the TRPM8 channel (10), but it now appears that analogous mutations do not have the same effects in other, related TRP channels.

Our results identified two charged residues within the S4/S4–S5 region, Arg^{557} and Asp^{576}, that are involved in the voltage-dependent gating of TRPV1. These residues, together with Glu^{570} and Arg^{579}, also contribute to the voltage modulation of the capsaicin-induced currents (Fig. 2*C*) and the capsaicin potentiation of the heat-induced currents (supplemental Fig. S3*B*). In E570Q and R579D, the voltages causing half-maximal activation ($V_{1/2}$) were identical to the wild type, but their voltage-independent components of capsaicin-induced activation were distinct and different from the wild

type. This might indicate that these two mutations at least partially uncouple voltage from chemical and thermal sensitivity. Consistent with these findings, a very recent study, comparing the energetics of thermal gating in absence and presence of membrane depolarization or chemical agonists, demonstrated that the activation of voltage sensors is not necessary for TRPV1 channel gating (30).

The putative structures of the S4–S5 region of TRPV1 predicted from the homology models published previously suggest the proximity of Arg^{557} to Glu^{570} (15, 18). Indeed, our functional data support a scenario in which Arg^{557} interacts with Glu^{570}. The partial recovery of the capsaicin-induced voltage-modulated activity (Fig. 3*C*) and potentiation of heat-evoked responses (supplemental Fig. S3*B*) by the charge-swapping mutation R557E/E570R indicates that an interaction between these two sites spaced 13 residues apart might contribute to allosteric coupling between the voltage-, temperature- and capsaicin-dependent activation mechanisms. This hypothesis is further supported by two other observations: We found that 1) an aromatic residue is required at position 554, and E570R, in the presence of capsaicin, exhibits a greater apparent gating valence z than the wild-type channel, indicative of an increased contribution to voltage sensing. Thus, it could be that the predicted energetically significant cation-π interaction between Tyr^{554} and Arg^{557} (less than −3.16 kcal/mol) contributes to channel activation and can be substituted by another cation-π interaction between Tyr^{554} and Arg^{570} (−1.03 kcal/mol) in the E570R mutant (see Ref. 31). In this regard, the involvement of the tyrosine and arginine at positions homologous to Tyr^{554} and Arg^{557} in a general gating mechanism had been proposed earlier for the related TRPV4 channel (32). 2) We also confirmed that the TRPV1 mutation G563S stabilizes the open conformation and leads to overactive channels (supplemental Fig. S4). The role of this glycine as a flexible hinge between S4 and the S4–S5 linker helices appears to be directly related to the changes in equilibrium between the open and closed states of the channel. This might be a plausible explanation for the total conservation of glycine at this position in the sequence of all TRPV channels.

Our experiments on systematically replacing Arg^{579} with alanine, glutamate, or aspartate, and the partial functional recovery of the double mutant D576R/R579E (supplemental Fig. S3*B*), indicate that the local charge distribution around these two residues is critical for the voltage and heat modulation of the capsaicin-activated states of the channel. Two other interesting features arise from our data: 1) a leftward shift in $V_{1/2}$ and strong changes in the capsaicin-induced activation/deactivation kinetics that was found for three distinct mutations distant in sequence: R557K, G563S, and for the previously reported gain-of-function mutant M581T (16), might support the proposed role of the S4/S4–S5 segment as a modular domain that, depending on the stimulus context, mediates the channel activation and/or deactivation. 2) The finding that K571E is normal in all aspects of TRPV1 modulation except for 2-APB responsiveness confirms that this mutant uncouples the 2-APB sensitivity from other TRPV1 modalities.

Surprisingly, we found out that TRPV3-Y565S responded normally to temperature and 2-APB, although the equivalent mutation led to a complete loss of function in TRPV1. Also, charge-replacing mutations, equivalent to the most affected mutations in TRPV1, left the heat- and 2-APB-induced activation unchanged in TRPV2 and TRPV3. In addition, neither the mutation hTRPV2-K527E nor the hTRPV3-K581E mutation, corresponding to rTRPV1-K571E, affected the 2-APB-dependent currents. Thus, our data indicate that the mechanisms of temperature, voltage, and chemical sensitivity in TRPV1, TRPV2, and TRPV3 might be dependent on distinct residues of the S4 and S4–S5 linker region, and, despite their highly conserved nature, they may be not fully conserved throughout these thermosensitive TRPV channels.

Acknowledgment—We thank M. Kuntosova for excellent technical assistance.

REFERENCES

1. Caterina, M. J., Schumacher, M. A., Tominaga, M., Rosen, T. A., Levine, J. D., and Julius, D. (1997) *Nature* **389,** 816–824
2. Voets, T., Droogmans, G., Wissenbach, U., Janssens, A., Flockerzi, V., and Nilius, B. (2004) *Nature* **430,** 748–754
3. Tominaga, M., Caterina, M. J., Malmberg, A. B., Rosen, T. A., Gilbert, H., Skinner, K., Raumann, B. E., Basbaum, A. I., and Julius, D. (1998) *Neuron* **21,** 531–543
4. Matta, J. A., and Ahern, G. P. (2007) *J. Physiol.* **585,** 469–482
5. Brauchi, S., Orio, P., and Latorre, R. (2004) *Proc. Natl. Acad. Sci. U.S.A.* **101,** 15494–15499
6. Latorre, R., Zaelzer, C., and Brauchi, S. (2009) *Q. Rev. Biophys.* **42,** 201–246
7. Bezanilla, F. (2008) *Nat. Rev. Mol. Cell Biol.* **9,** 323–332
8. Villalba-Galea, C. A., Sandtner, W., Starace, D. M., and Bezanilla, F. (2008) *Proc. Natl. Acad. Sci. U.S.A.* **105,** 17600–17607
9. Long, S. B., Campbell, E. B., and MacKinnon, R. (2005) *Science* **309,** 903–908
10. Voets, T., Owsianik, G., Janssens, A., Talavera, K., and Nilius, B. (2007) *Nat. Chem. Biol.* **3,** 174–182
11. Nilius, B., Talavera, K., Owsianik, G., Prenen, J., Droogmans, G., and Voets, T. (2005) *J. Physiol.* **567,** 35–44
12. Susankova, K., Ettrich, R., Vyklicky, L., Teisinger, J., and Vlachova, V. (2007) *J. Neurosci.* **27,** 7578–7585
13. Vlachová, V., Teisinger, J., Susánková, K., Lyfenko, A., Ettrich, R., and Vyklický, L. (2003) *J. Neurosci.* **23,** 1340–1350
14. Dittert, I., Benedikt, J., Vyklický, L., Zimmermann, K., Reeh, P. W., and Vlachová, V. (2006) *J. Neurosci. Methods* **151,** 178–185
15. Brauchi, S., Orta, G., Mascayano, C., Salazar, M., Raddatz, N., Urbina, H., Rosenmann, E., Gonzalez-Nilo, F., and Latorre, R. (2007) *Proc. Natl. Acad. Sci. U.S.A.* **104,** 10246–10251
16. Myers, B. R., Bohlen, C. J., and Julius, D. (2008) *Neuron* **58,** 362–373
17. Xiao, R., Tian, J., Tang, J., and Zhu, M. X. (2008) *Cell Calcium* **43,** 334–343
18. Fernández-Ballester, G., and Ferrer-Montiel, A. (2008) *J. Membr. Biol.* **223,** 161–172
19. Novakova-Tousova, K., Vyklicky, L., Susankova, K., Benedikt, J., Samad, A., Teisinger, J., and Vlachova, V. (2007) *Neuroscience* **149,** 144–154
20. Yao, J., and Qin, F. (2009) *PLoS Biol.* **7,** e46
21. Hu, H. Z., Gu, Q., Wang, C., Colton, C. K., Tang, J., Kinoshita-Kawada, M., Lee, L. Y., Wood, J. D., and Zhu, M. X. (2004) *J. Biol. Chem.* **279,** 35741–35748
22. Chung, M. K., Lee, H., Mizuno, A., Suzuki, M., and Caterina, M. J. (2004) *J. Neurosci.* **24,** 5177–5182
23. Hu, H., Grandl, J., Bandell, M., Petrus, M., and Patapoutian, A. (2009)

Proc. Natl. Acad. Sci. U.S.A. **106,** 1626–1631
24. Neeper, M. P., Liu, Y., Hutchinson, T. L., Wang, Y., Flores, C. M., and Qin, N. (2007) *J. Biol. Chem.* **282,** 15894–15902
25. Asakawa, M., Yoshioka, T., Matsutani, T., Hikita, I., Suzuki, M., Oshima, I., Tsukahara, K., Arimura, A., Horikawa, T., Hirasawa, T., and Sakata, T. (2006) *J. Invest. Dermatol.* **126,** 2664–2672
26. Jordt, S. E., and Julius, D. (2002) *Cell* **108,** 421–430
27. Gavva, N. R., Klionsky, L., Qu, Y., Shi, L., Tamir, R., Edenson, S., Zhang, T. J., Viswanadhan, V. N., Toth, A., Pearce, L. V., Vanderah, T. W., Porreca, F., Blumberg, P. M., Lile, J., Sun, Y., Wild, K., Louis, J. C., and Treanor, J. J. (2004) *J. Biol. Chem.* **279,** 20283–20295
28. Grandl, J., Hu, H., Bandell, M., Bursulaya, B., Schmidt, M., Petrus, M., and Patapoutian, A. (2008) *Nat. Neurosci.* **11,** 1007–1013
29. Yang, F., Cui, Y., Wang, K., and Zheng, J. (2010) *Proc. Natl. Acad. Sci. U.S.A.* **107,** 7083–7088
30. Yao, J., Liu, B., and Qin, F. (2010) *Biophys. J.* **99,** 1743–1753
31. Gallivan, J. P., and Dougherty, D. A. (1999) *Proc. Natl. Acad. Sci. U.S.A.* **96,** 9459–9464
32. Vriens, J., Owsianik, G., Janssens, A., Voets, T., and Nilius, B. (2007) *J. Biol. Chem.* **282,** 12796–12803